T-odd proton-helicity asymmetry in semi-inclusive DIS in perturbative QCD

Maurizio Abele,[1] Matthias Aicher,[2] Fulvio Piacenza,[3] Andreas Schäfer,[2] and Werner Vogelsang[1]
[1]*Institute for Theoretical Physics, Tübingen University, Auf der Morgenstelle 14, 72076 Tübingen, Germany*
[2]*Institut für Theoretische Physik, Universität Regensburg, 93040 Regensburg, Germany*
[3]*Dipartimento di Fisica, Università di Pavia, via Bassi 6, 27100 Pavia, Italy*

(Received 3 May 2022; accepted 9 July 2022; published 25 July 2022)

We compute the single-spin asymmetry A_{UL} in semi-inclusive deep-inelastic scattering of unpolarized leptons and longitudinally polarized protons at a large transverse momentum of the produced hadron. Our calculation is performed in collinear factorization at the lowest order of QCD perturbation theory. For photon exchange, the asymmetry is T-odd and receives contributions from the interference of the tree level and one-loop absorptive amplitudes. We consider the behavior of the spin asymmetry at low transverse momentum where contact to the formalism based on transverse momentum dependent distribution functions can be made. We also present some phenomenological results relevant for the COMPASS and HERMES experiments and the future Electron-Ion Collider.

DOI: 10.1103/PhysRevD.106.014020

I. INTRODUCTION

T-odd effects in semi-inclusive deep-inelastic scattering (SIDIS) have been a focus of numerous theoretical and experimental studies in recent years [1]. These studies were motivated by the discovery [2–4] that a proton can in fact have intrinsic T-odd parton distribution functions, associated with the interplay of transverse polarization of the proton or its partons with the partonic transverse momenta. Here, the term "T-odd" refers to a "naive" time-reversal operation, which corresponds to ordinary time reversal without the interchange of initial and final states of the reaction considered.

T-odd effects can, however, also be generated in perturbation theory. They are absent at tree level, but the seminal papers [5–10] described how they can arise from absorptive parts of loop amplitudes at $\mathcal{O}(\alpha_s^2)$ in QCD hard scattering, where α_s is the strong coupling. Initially proposed as tests of QCD and its gluon self-coupling [6,7,9], T-odd effects in perturbative QCD have remained a subject of interest ever since [11–21]. In regards to SIDIS, the early studies [10,16,17] have addressed neutrino scattering as well as scattering of longitudinally polarized leptons off unpolarized protons [16,17].

In the present paper, we extend the previous work and compute the leading perturbative T-odd effects for SIDIS with unpolarized leptons colliding with longitudinally polarized protons via photon exchange [22–24], which, to our knowledge, have not been investigated by other authors. Calculating the relevant absorptive parts of one-loop amplitudes and using collinear factorization, we derive the corresponding azimuthal terms in the spin asymmetry A_{UL} when the proton beam helicity is flipped. Our calculation is to be seen in the same spirit as other approaches that aim to obtain the phase required for (in their case, transverse) single-spin asymmetries through a hard-scattering mechanism [20,21,25]. In particular, Ref. [21] has investigated perturbative T-odd effects for the single- *transverse* SIDIS spin asymmetry A_{UT} via the structure function g_T, and, as we shall see, there are interesting connections of that study to our present work.

There are several aspects of this observable that motivate us to carry out this study. First, and perhaps foremost, perturbative T-odd effects in QCD have remained elusive so far, and, given their unique property of arising from loop effects in QCD, any observable sensitive to them is valuable. In this context, it is also worth mentioning that for A_{UL}, the effects are sensitive to the proton's helicity parton distributions *despite* the fact that an unpolarized lepton beam is used. This is quite unique as well since usually conservation of parity in strong interactions prohibits such single-longitudinal spin asymmetries.

Second, measurements of the relevant azimuthal terms have been carried out in various fixed-target experiments by the HERMES [26–29], CLAS [30], and COMPASS [31–33] collaborations, albeit in kinematic regions that are not clearly in the perturbative regime. Nevertheless, it is interesting to see whether the perturbative calculations give

results that are roughly consistent with data at the highest transverse momenta $P_{h\perp}$ of the produced hadron accessed so far. Much higher $P_{h\perp}$ should become available at the future Electron-Ion Collider (EIC), where SIDIS studies with exquisite precision will be feasible [34]. It is therefore valuable to extend the "library" of observables relevant at the EIC.

Finally, as mentioned above, most studies of T-odd effects in QCD have addressed the nonperturbative regime in terms of parton distributions and fragmentation functions. For SIDIS, this approach becomes particularly useful when the transverse momentum of the outgoing hadron is relatively low, $P_{h\perp}^2 \ll Q^2$, with Q^2 the virtuality of the exchanged photon. In this case, one can describe SIDIS in terms of "transverse momentum dependent" (TMD) parton distributions and fragmentation functions [35,36]. As has been shown [37,38], TMDs can indeed generate the SIDIS spin asymmetry A_{UL}, and numerous phenomenological studies have been performed [39–46]. Having also a perturbative calculation of A_{UL}, for which the observed transverse momentum is acquired by the recoil against a hard parton in the scattering process, one can address the question in how far the TMD formalism is recovered as one takes the limit $P_{h\perp}^2 \ll Q^2$. General statements about the high-transverse-momentum tail of TMDs were developed in [47], which also make predictions for the behavior of A_{UL} that may be directly compared to our results. In this context, the T-odd beam-spin asymmetry A_{LU} is also interesting [16,17,48,49], for which the initial lepton is polarized, and we will briefly discuss this asymmetry as well. We note that additional insights into the matching of TMDs to perturbative calculations have become available in recent years [50–59].

Our paper is organized as follows. In Sec. II, we introduce the kinematic variables and the main ingredients for the perturbative description of the spin-dependent SIDIS cross section. In Sec. III, we briefly review the main properties of T-odd asymmetries and describe the strategy for our calculation. Section IV presents our perturbative results for the T-odd contributions to the SIDIS spin asymmetry. Next, in Sec. V, we consider the limit of small transverse momenta and compare to known results in the TMD regime. Phenomenological results are presented in Sec. VI. Here, we consider the spin asymmetry A_{UL} at the EIC and also compare to the COMPASS [31] and HERMES data [26,29]. Section VII concludes our paper.

II. PERTURBATIVE SIDIS CROSS SECTION

We consider the SIDIS process,

$$\ell(k) + p(P,S) \to \ell'(k') + h(P_h) + X,$$

where we have indicated the four-momenta of the participating particles, and where S is the proton spin vector. We set $q \equiv k - k'$ and $Q^2 \equiv -q^2$ for the exchanged virtual gauge boson, for which we will consider only a virtual photon, thus excluding parity-violating effects. The usual kinematical variables relevant for SIDIS are defined as

$$x = \frac{Q^2}{2P\cdot q}, \qquad y = \frac{P\cdot q}{P\cdot k}, \qquad z = \frac{P\cdot P_h}{P\cdot q}. \tag{1}$$

In the following, we will consider the transverse momentum $P_{h\perp}$ and its azimuthal angle ϕ_h with respect to the lepton plane, defined in a suitable reference frame. For SIDIS phenomenology, one usually adopts the proton rest frame. The kinematics of the process in this frame are depicted on the left side of Fig. 1. The x_3 axis is defined by the direction of the photon three-momentum $\vec{q}$. Our actual calculations will be performed in the Breit frame in which the photon four-momentum has a vanishing energy component, $q = (0,0,0,Q)$, which simplifies the calculations. This frame is related to the rest frame by a longitudinal boost along the x_3 axis so that all transverse components remain unchanged. The situation in the Breit frame is shown on the right side of Fig. 1.

As discussed in the Introduction, we consider longitudinal polarization for the proton. In the proton rest frame, this is defined by choosing the proton's spin vector along (or opposite to) the direction of the virtual photon. Here, $\vec{S}\|\vec{q}$ will correspond to negative longitudinal polarization of the proton. We note that in actual experiments, one will define longitudinal polarization in the proton rest frame by choosing the spin parallel or antiparallel to the *lepton* beam direction rather than the photon one. The two cases are, of course, related; all details may be found in Ref. [60] (see also [29]). Specifically, they differ by admixtures related to the corresponding transverse single-spin asymmetry A_{UT}, which can be taken into account in the experimental analysis. Note that the case with polarization along the lepton beam direction readily extends to the situation at an ℓp collider, where a longitudinally polarized proton will be in a helicity state. In the following, we will therefore consider protons with either positive or negative helicity.

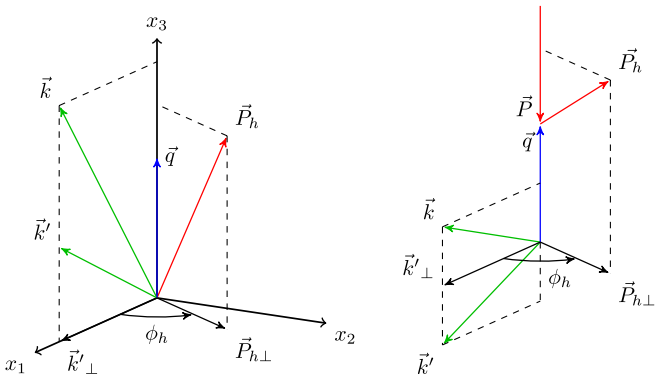

FIG. 1. Left: Kinematics of the SIDIS process in the rest frame of the proton. Right: Same in the Breit frame.

For an incoming unpolarized lepton scattering off a longitudinally polarized proton, two independent structure functions contribute to the proton helicity-dependent part of the cross section [38,47,61], entering with dependencies of the form $\sin(\phi_h)$ or $\sin(2\phi_h)$, respectively. Explicitly, we have

$$\frac{d^5\Delta\sigma^h}{dxdydzdP_{h\perp}^2 d\phi_h} = \frac{1}{2}\left(\frac{d^5\sigma_+^h}{dxdydzdP_{h\perp}^2 d\phi_h} - \frac{d^5\sigma_-^h}{dxdydzdP_{h\perp}^2 d\phi_h}\right) = \frac{\pi\alpha^2}{xQ^2}\frac{y}{1-\varepsilon}\left\{\sqrt{2\varepsilon(1+\varepsilon)}F_{\mathrm{UL}}^{\sin\phi_h}\sin(\phi_h) + \varepsilon F_{\mathrm{UL}}^{\sin 2\phi_h}\sin(2\phi_h)\right\}, \tag{2}$$

where the subscripts $\pm$ denote proton helicities, and ε is defined as the ratio of longitudinal and transverse photon fluxes,

$$\varepsilon \equiv \frac{1-y}{1-y+y^2/2}. \tag{3}$$

The structure functions $F_{\mathrm{UL}}^{\sin\phi_h}, F_{\mathrm{UL}}^{\sin 2\phi_h}$ depend on x, z, Q^2, and $P_{h\perp}^2$, which we will usually not write out. In the following, we will compute them in collinear factorization, where they become double convolutions of helicity parton distribution functions, fragmentation functions, and perturbative partonic coefficient functions. We will only consider the lowest order (LO) in perturbation theory, at which the structure functions may be cast into the forms,

$$F_{\mathrm{UL}}^{\sin\phi_h} = \left(\frac{\alpha_s(\mu^2)}{2\pi}\right)^2 \frac{x}{Q^2 z^2}\sum_{\substack{a,b\\=q,\bar{q},g}}\int_x^1\frac{d\hat{x}}{\hat{x}}\int_z^1\frac{d\hat{z}}{\hat{z}}\Delta f_a\left(\frac{x}{\hat{x}},\mu^2\right)C_{\mathrm{UL}}^{\sin\phi_h,a\to b}(\hat{x},\hat{z})D_b^h\left(\frac{z}{\hat{z}},\mu^2\right)\delta\left(\frac{q_T^2}{Q^2}-\frac{(1-\hat{x})(1-\hat{z})}{\hat{x}\,\hat{z}}\right), \tag{4}$$

and likewise for $F_{\mathrm{UL}}^{\sin 2\phi_h}$. The factor $(\alpha_s/(2\pi))^2 x/(Q^2 z^2)$ has been introduced for convenience; it explicitly exhibits the leading power of α_s of the structure functions and also makes the coefficient functions $C_{\mathrm{UL}}^{\sin\phi_h,a\to b}$, $C_{\mathrm{UL}}^{\sin 2\phi_h,a\to b}$ dimensionless functions of only the two partonic variables,

$$\hat{x} \equiv \frac{Q^2}{2p_a\cdot q}, \qquad \hat{z} \equiv \frac{p_a\cdot p_b}{p_a\cdot q}, \tag{5}$$

which are the partonic counterparts of the hadronic variables in Eq. (1). The coefficient functions are to be derived for each $2\to 2$ partonic channel $\gamma^* + a \to b + c$, where parton b fragments into the observed hadron, and parton c remains unobserved. These processes are $\gamma^* q(\bar{q}) \to q(\bar{q})g$, $\gamma^* q(\bar{q}) \to gq(\bar{q})$, $\gamma^* g \to q\bar{q}$, and $\gamma^* g \to \bar{q}q$.

In Eq. (4), $\Delta f_a(\xi,\mu^2)$ is the helicity distribution of parton $a = q, \bar{q}, g$ in the proton at momentum fraction ξ and factorization scale μ (which, for simplicity, we choose equal to the renormalization scale μ appearing in the strong coupling constant α_s). Furthermore, $D_b^h(\zeta,\mu^2)$ is the corresponding fragmentation function for parton b going to the observed hadron h, at momentum fraction ζ and, again, at factorization scale μ. All functions in Eq. (4) are tied together by the δ function in the second line, which expresses the fact that at LO, the recoiling partonic system consists of a single massless parton c. For convenience, we have introduced the variable,

$$q_T^2 \equiv \frac{P_{h\perp}^2}{z^2}. \tag{6}$$

III. T-ODD SINGLE-SPIN ASYMMETRY AT LOWEST ORDER

The terms proportional to $\sin(\phi_h)$ and $\sin(2\phi_h)$ represent correlations of the forms, $\vec{S}\cdot(\vec{k}'_\perp\times\vec{P}_{h\perp})$ and $\vec{S}\cdot(\vec{k}'_\perp\times\vec{P}_{h\perp})(\vec{k}'_\perp\cdot\vec{P}_{h\perp})$, respectively, which already suggests that they are "naively" time-reversal odd. This sets a constraint on the partonic scattering processes that may contribute to the corresponding asymmetries in perturbation theory. To set the stage for our derivations, we briefly review how this constraint can be exploited to simplify the calculations.

Denoting as S_{fi} the scattering matrix element between an initial state i and a final state f, a *naive* time-reversal transformation corresponds to a time-reversal without interchange of initial and final states. Hence, a T-odd observable is characterized by [10,62,63]

$$|S_{fi}|^2 \neq |S_{\tilde{f}\tilde{i}}|^2, \tag{7}$$

where $\tilde{i}(\tilde{f})$ is obtained from $i(f)$ by reversing momenta and spins. T-odd effects can also be present in theories that are invariant under *true* time-reversal, fulfilling

$$|S_{fi}|^2 = |S_{\tilde{i}\tilde{f}}|^2. \tag{8}$$

This is easily understood by considering the reaction matrix T:

$$S_{fi} \equiv \delta_{fi} + i(2\pi)^4\delta^{(4)}(P_f - P_i)T_{fi}, \tag{9}$$

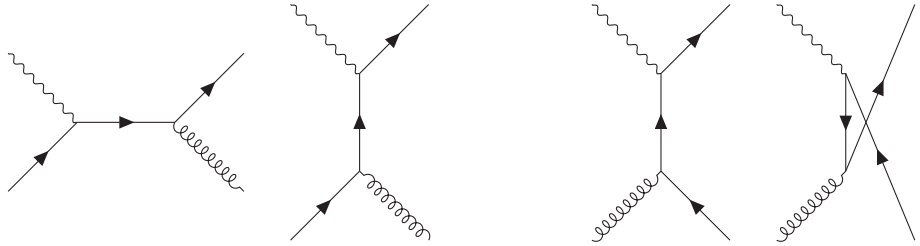

FIG. 2. Tree-level diagrams for $\gamma^* + q \to q + g$ and $\gamma^* + g \to q + \bar{q}$.

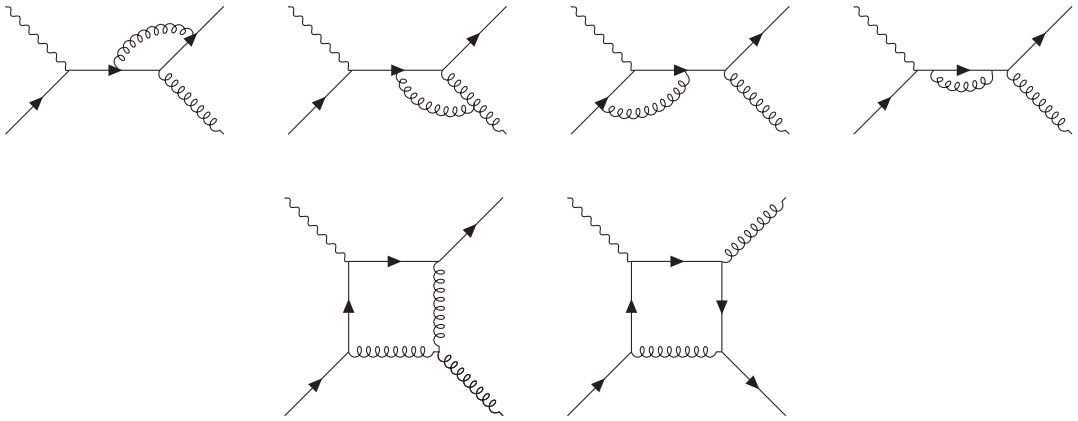

FIG. 3. One-loop diagrams for $\gamma^* + q \to q + g$ that provide a phase relative to the tree-level amplitude. We note that there are additional one-loop diagrams that do not produce a phase.

and the unitarity condition for the scattering matrix,

$$T_{fi} - T^*_{if} = i\sum_X T^*_{Xf} T_{Xi} \delta^{(4)}(P_X - P_i) \equiv i\alpha_{fi}, \qquad (10)$$

where, in the last equation, we introduced the absorptive part α_{fi} of the reaction amplitude. Equation (10) can be rewritten as $T^*_{if} = T_{fi} - i\alpha_{fi}$. Taking the square modulus of both sides, we find

$$|T_{if}|^2 = |T_{fi}|^2 + 2\,\mathrm{Im}(T^*_{fi}\alpha_{fi}) + |\alpha_{fi}|^2. \qquad (11)$$

True time reversal invariance, Eq. (8), implies $|T_{if}|^2 = |T_{\tilde{f}\tilde{i}}|^2$ (leaving aside the case $i = f$). Thus, if only QED and QCD interactions are present, Eq. (11) gives an expression for T-odd terms:

$$|T_{\tilde{f}\tilde{i}}|^2 - |T_{fi}|^2 = 2\mathrm{Im}(T^*_{fi}\alpha_{fi}) + |\alpha_{fi}|^2. \qquad (12)$$

If we consider the partonic processes underlying semi-inclusive DIS, the LO contributions to T_{fi} are the tree-level diagrams for $\gamma^* + q \to q + g$ and $\gamma^* + g \to q + \bar{q}$ shown in Fig. 2. The leading terms for the absorptive amplitude α_{fi} arise from loop corrections already at one-loop order. The one-loop diagrams shown in Fig. 3 for the initial-quark channel and in Fig. 4 for the initial-gluon channel all have the property that they have an imaginary part and hence, produce a phase relative to the corresponding tree-level amplitudes. As a result, the term $2\mathrm{Im}(T^*_{fi}\alpha_{fi})$ in Eq. (12) is nonvanishing already due to the interferences of the one-loop and tree amplitudes. We conclude that LO contributions to T-odd effects in SIDIS come precisely from these interferences and are of order $\mathcal{O}(\alpha_s^2)$ [10].

Let us briefly describe the strategy we have adopted in computing the T-odd interference contributions. Introducing the amplitudes $\mathcal{M}^{\pm}_{ab}$ for positive and negative helicity of parton a in the channel $\gamma^* + a \to b + c$, we write the difference of their squares as

$$|\mathcal{M}^+_{ab}|^2 - |\mathcal{M}^-_{ab}|^2 = L^{\mu\nu}(\hat{W}^+_{\mu\nu} - \hat{W}^-_{\mu\nu}) \equiv L^{\mu\nu}\Delta\hat{W}_{\mu\nu}, \qquad (13)$$

where

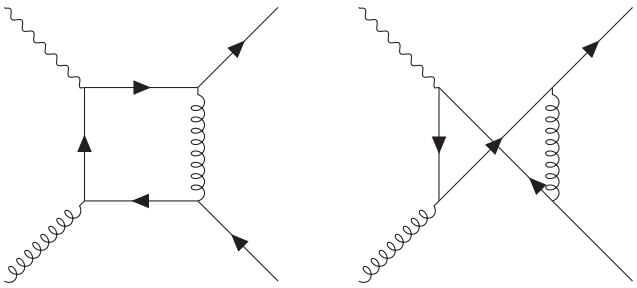

FIG. 4. One-loop diagrams for $\gamma^* + g \to q + \bar{q}$ that provide a phase relative to the tree-level amplitude.

$$L_{\mu\nu} = 2\left(k_\mu k'_\nu + k_\nu k'_\mu - \frac{Q^2}{2} g_{\mu\nu}\right) \tag{14}$$

is the leptonic tensor, and

$$\Delta\hat{W}_{\mu\nu} \equiv \langle p_a, +|J_\mu(0)|p_b p_c\rangle\langle p_b p_c|J_\nu(0)|p_a, +\rangle - \langle p_a, -|J_\mu(0)|p_b p_c\rangle\langle p_b p_c|J_\nu(0)|p_a, -\rangle \tag{15}$$

is the partonic tensor for a polarized parton a in the initial state and a fragmenting parton b in the final state (at LO, the final state is completely fixed by a and b). Since, as discussed above, only interferences between tree-level and one-loop amplitudes contribute to the order we are considering, we have

$$\Delta\hat{W}_{\mu\nu} = [\langle p_a, +|J_{\mu,\text{tree}}(0)|p_b p_c\rangle\langle p_b p_c|J_{\nu,\text{loop}}(0)|p_a, +\rangle + \langle p_a, +|J_{\mu,\text{loop}}(0)|p_b p_c\rangle\langle p_b p_c|J_{\nu,\text{tree}}(0)|p_a, +\rangle] - [\langle p_a, -|J_{\mu,\text{tree}}(0)|p_b p_c\rangle\langle p_b p_c|J_{\nu,\text{loop}}(0)|p_a, -\rangle + \langle p_a, -|J_{\mu,\text{loop}}(0)|p_b p_c\rangle\langle p_b p_c|J_{\nu,\text{tree}}(0)|p_a, -\rangle]. \tag{16}$$

The phase required for a nonvanishing imaginary part is generated by analytic continuation of logarithms in the loop integrals, e.g.,

$$\ln\left(-\frac{\mu^2}{\hat{s} + i\epsilon}\right) \to \ln\left(\frac{\mu^2}{\hat{s}}\right) + i\pi, \tag{17}$$

where $\hat{s} = (q+p)^2 = Q^2(1-\hat{x})/\hat{x}$. As mentioned, such phases only appear in the s-channel diagrams and the two box-diagrams in Fig. 3 for initial quarks (or antiquarks). For initial gluons, they appear in the two box diagrams in Fig. 4.

It is quite straightforward to compute the partonic tensor $\Delta\hat{W}_{\mu\nu}$. The only subtlety is related to the use of the Dirac matrix γ_5 and the Levi-Civita tensor $\varepsilon_{\mu\nu\rho\sigma}$ in dimensional regularization in $d = 4 - 2\epsilon$ dimensions. Here, we have used the scheme of Refs. [64,65], which is known to be algebraically consistent. We have used the MATHEMATICA package TRACER [66] to compute the Dirac traces and contractions and PACKAGE-X [67] for the evaluation of the loop integrals and their imaginary parts. We note that poles in $\epsilon = 0$ arise at various intermediate stages of the calculation; these all have to cancel in the end since, at the lowest order, the T-odd part of the hadronic tensor must not have any ultraviolet or infrared or collinear singularities. This provides a useful check on our calculation. The partonic coefficient functions are found from the final result for $L^{\mu\nu}\Delta\hat{W}_{\mu\nu}$ as the coefficients of the terms $\sim\sin(\phi_h)$ and $\sim\sin(2\phi_h)$. No other angular dependencies appear.

IV. ANALYTICAL RESULTS

For the partonic coefficient functions for $F_{\text{UL}}^{\sin\phi_h}$, we find [23,24]

$$\begin{aligned}
C_{\text{UL}}^{\sin\phi_h, q\to q}(\hat{x},\hat{z}) &= e_q^2 C_F\left(C_A(1-\hat{x}) + C_F(\hat{x} - 1 - \hat{z} + 3\hat{x}\,\hat{z}) + (C_A - 2C_F)(1-2\hat{x})\frac{\hat{z}\ln\hat{z}}{1-\hat{z}}\right)\frac{Q}{q_T},\\
C_{\text{UL}}^{\sin\phi_h, q\to g}(\hat{x},\hat{z}) &= -e_q^2 C_F\frac{(1-\hat{z})}{\hat{z}}\left(C_A(1-\hat{x}) + C_F(-3\hat{x}\,\hat{z} + 4\hat{x} + \hat{z} - 2) + (C_A - 2C_F)(1-2\hat{x})\frac{(1-\hat{z})\ln(1-\hat{z})}{\hat{z}}\right)\frac{Q}{q_T},\\
C_{\text{UL}}^{\sin\phi_h, g\to q}(\hat{x},\hat{z}) &= e_q^2(C_A - 2C_F)(1-\hat{x})\frac{1}{2\hat{z}^2}\left(\hat{x}\,\hat{z}(1-2\hat{z}) - (1-\hat{x})\ln(1-\hat{z}) + (1-\hat{x})\frac{\hat{z}\ln(\hat{z})}{1-\hat{z}}\right)\frac{Q}{q_T},
\end{aligned} \tag{18}$$

while for the coefficients for $F_{\text{UL}}^{\sin 2\phi_h}$, we have [23,24]

$$\begin{aligned}
C_{\text{UL}}^{\sin 2\phi_h, q\to q}(\hat{x},\hat{z}) &= e_q^2 C_F(1-\hat{x})\left((C_A - 2C_F)\frac{(1-2\hat{z})\ln\hat{z}}{1-\hat{z}} - (C_A + (1-3\hat{z})C_F)\right)\frac{Q^2}{q_T^2},\\
C_{\text{UL}}^{\sin 2\phi_h, q\to g}(\hat{x},\hat{z}) &= -e_q^2 C_F(1-\hat{x})\frac{(1-\hat{z})^2}{\hat{z}^2}\left((C_A - 2C_F)\frac{(1-2\hat{z})\ln(1-\hat{z})}{\hat{z}} + (C_A - (2-3\hat{z})C_F)\right)\frac{Q^2}{q_T^2},\\
C_{\text{UL}}^{\sin 2\phi_h, g\to q}(\hat{x},\hat{z}) &= e_q^2(C_A - 2C_F)(1-\hat{x})^2\frac{1}{2\hat{z}^3}\left(\hat{z}(2(1-\hat{z})\hat{z} - 1) - (1-\hat{z})\ln(1-\hat{z}) - \frac{\hat{z}^2\ln\hat{z}}{1-\hat{z}}\right)\frac{Q^2}{q_T^2}.
\end{aligned} \tag{19}$$

Note that the ratio q_T/Q in the above expressions is fixed by $\hat{x}$ and $\hat{z}$ through the δ-function in (4). The $q \to q$ and $q \to g$ coefficients are related by crossing symmetry in the following way:

$$C_{\rm UL}^{\sin\phi_h,q\to g}(\hat{x},\hat{z}) = -C_{\rm UL}^{\sin\phi_h,q\to q}(\hat{x},1-\hat{z}),$$
$$C_{\rm UL}^{\sin 2\phi_h,q\to g}(\hat{x},\hat{z}) = C_{\rm UL}^{\sin 2\phi_h,q\to q}(\hat{x},1-\hat{z}). \tag{20}$$

Furthermore, because of charge conjugation and parity invariance, the results for the antiquark channels $\bar{q}\to\bar{q}$ and $\bar{q}\to g$ are identical to those for $q\to q$ and $q\to g$, respectively. In addition, we have

$$C_{\rm UL}^{\sin\phi_h,g\to\bar{q}}(\hat{x},\hat{z}) = -C_{\rm UL}^{\sin\phi_h,g\to q}(\hat{x},1-\hat{z}),$$
$$C_{\rm UL}^{\sin 2\phi_h,g\to\bar{q}}(\hat{x},\hat{z}) = C_{\rm UL}^{\sin 2\phi_h,g\to q}(\hat{x},1-\hat{z}). \tag{21}$$

In Ref. [22], we have also derived these results via crossing of the corresponding T-odd asymmetries in e^+e^- annihilation in [17]. Our results given above correct the sign of the results in [22]. For the case of quark-initiated processes, an independent cross-check is provided by the SIDIS beam asymmetries $A_{\rm LU}$ calculated in Ref. [10]. Indeed, for the charged-current case considered in these papers, the interaction mediated by W bosons selects left-handed quarks so that even if the target is unpolarized, the partonic matrix elements are the same as in our Eq. (16), albeit with reversed helicity. For instance, by looking at the functions F_8 and F_9 in Eqs. (3.14) of [17], in the case of quark-initiated diagrams, one can verify that they correspond to our $C_{\rm UL}^{\sin\phi_h}$ and $C_{\rm UL}^{\sin 2\phi_h}$ functions with a reversed sign. Clearly, this reasoning does not allow comparisons in the case of incoming gluons.

As we mentioned in the Introduction, there are interesting connections of our work to the recent study [21] on a two-loop perturbative mechanism for the single-transverse SIDIS spin asymmetry $A_{\rm UT}$ involving the structure function g_T. A well-known feature of g_T is that its Wandzura-Wilczek [68] part is proportional to an integral over the quark and gluon helicity parton distributions. This part of the calculation of [21] therefore involves hard-scattering cross sections with definite helicities of the incoming partons. Remarkably, these turn out to be the same as the ones we have presented above (apart, of course, from normalization, which is necessarily different for $A_{\rm UL}$ and $A_{\rm UT}$). This feature deserves further investigation in the future.

V. LOW-q_T LIMIT

As discussed in the Introduction, it is interesting to expand the above results for the structure functions for low values of q_T/Q, in order to make contact with results predicted by the TMD formalism. When $q_T^2/Q^2\to 0$, we can expand the delta condition in (4) as described, for example, in [69–71]:

$$\frac{1}{\hat{x}\,\hat{z}}\delta\left(\frac{q_T^2}{Q^2}-\frac{(1-\hat{x})(1-\hat{z})}{\hat{x}\,\hat{z}}\right) = \delta(1-\hat{z})\delta(1-\hat{x})\ln\left(\frac{Q^2}{q_T^2}\right)+\frac{\delta(1-\hat{z})}{(1-\hat{x})_+}+\frac{\delta(1-\hat{x})}{(1-\hat{z})_+}+\mathcal{O}\left(\frac{q_T^2}{Q^2}\right). \tag{22}$$

Here, the "plus" distribution is defined in the usual way upon integration with a regular function:

$$\int_0^1 dy(f(y))_+ g(y) \equiv \int_0^1 dy f(y)(g(y)-g(1)). \tag{23}$$

To simplify notation, we write the double convolution integral as (we omit the scale dependence of the parton distributions and fragmentation functions here):

$$(\Delta f\otimes\mathcal{C}\otimes D)(x,z) \equiv \int_x^1\frac{d\hat{x}}{\hat{x}}\int_z^1\frac{d\hat{z}}{\hat{z}}\delta\left(\frac{q_T^2}{Q^2}-\frac{(1-\hat{x})(1-\hat{z})}{\hat{x}\,\hat{z}}\right)\Delta f\left(\frac{x}{\hat{x}}\right)\mathcal{C}(\hat{x},\hat{z})D\left(\frac{z}{\hat{z}}\right). \tag{24}$$

From the $\sin(\phi_h)$ terms in (18), we then find the following contribution to the $q\to q$ coefficient at low q_T/Q:

$$(\Delta f_q\otimes C_{\rm UL}^{\sin\phi_h,q\to q}\otimes D_q^h)(x,z) = e_q^2\frac{Q}{q_T}\frac{C_A}{2}\left\{-C_F\left(2\ln\left(\frac{q_T^2}{Q^2}\right)+3\right)\Delta f_q(x)D_q^h(z)+D_q^h(z)\int_x^1 d\hat{x}\,\delta P_{qq}(\hat{x})\Delta f_q\left(\frac{x}{\hat{x}}\right)\right.$$
$$\left.+\Delta f_q(x)\int_z^1 d\hat{z}\,\delta P_{qq}(\hat{z})D_q^h\left(\frac{z}{\hat{z}}\right)\right\}-e_q^2\frac{Q}{q_T}\frac{C_F}{C_A}\Delta f_q(x)\int_z^1 d\hat{z}\frac{\hat{z}}{1-\hat{z}}\left(1+\frac{\ln\hat{z}}{1-\hat{z}}\right)D_q^h\left(\frac{z}{\hat{z}}\right), \tag{25}$$

where

$$\delta P_{qq}(x) \equiv C_F\left[\frac{2x}{(1-x)_+}+\frac{3}{2}\delta(1-x)\right] \tag{26}$$

is the LO splitting function for the scale evolution of the transversity distributions. In the $q \to g$ channel, we obtain

$$(\Delta f_q \otimes C_{\rm UL}^{\sin\phi_h, q\to g} \otimes D_g^h)(x,z) = e_q^2 \frac{Q}{q_T} C_F \Delta f_q(x) \int_z^1 d\hat{z} \frac{1-\hat{z}}{\hat{z}^2} ((C_A - 2C_F)\ln(1-\hat{z}) - 2C_F\hat{z}) D_g^h\left(\frac{z}{\hat{z}}\right). \tag{27}$$

For the process $\gamma^* g \to q\bar{q}$, the coefficient function diverges logarithmically for $\hat{z} \to 1$. In addition to the expansion (22), we therefore also need

$$\begin{aligned}\frac{\ln(1-\hat{z})}{\hat{x}\,\hat{z}} \delta\left(\frac{q_T^2}{Q^2} - \frac{(1-\hat{x})(1-\hat{z})}{\hat{x}\,\hat{z}}\right) &= -\frac{1}{2}\ln^2\left(\frac{Q^2}{q_T^2}\right)\delta(1-\hat{x})\delta(1-\hat{z}) - \frac{\delta(1-\hat{z})}{(1-\hat{x})_+}\ln\left(\frac{Q^2}{q_T^2}\right) \\ &\quad + \delta(1-\hat{x})\left(\frac{\ln(1-\hat{z})}{1-\hat{z}}\right)_+ - \delta(1-\hat{z})\left(\left(\frac{\ln(1-\hat{x})}{1-\hat{x}}\right)_+ - \frac{\ln\hat{x}}{1-\hat{x}}\right).\end{aligned} \tag{28}$$

Details of the derivation of this equation are given in Appendix A. We then find

$$(\Delta f_g \otimes C_{\rm UL}^{\sin\phi_h, g\to q} \otimes D_q^h)(x,z)] = \frac{e_q^2}{2}\frac{Q}{q_T}(C_A - 2C_F) D_q^h(z) \int_x^1 d\hat{x}\, \Delta f_g\left(\frac{x}{\hat{x}}\right)\left[(1-\hat{x})\ln\left(\frac{Q^2}{q_T^2}\right) + (1-\hat{x})\ln\left(\frac{1-\hat{x}}{\hat{x}}\right) - 1\right]. \tag{29}$$

The results in Eqs. (25), (27), and (29) are valid up to terms of order q_T/Q. Keeping in mind the overall factor $1/Q^2$ in Eq. (4), we see that the structure function $F_{\rm UL}^{\sin\phi_h}$ is predicted to have the leading power,

$$F_{\rm UL}^{\sin\phi_h} \propto \frac{1}{Q q_T} + \mathcal{O}\left(\frac{1}{Q^2}\right), \tag{30}$$

at low q_T, modulo logarithms. The behavior found for $\gamma^* q \to qg$ in Eq. (25) is particularly interesting. The term $-C_F(2\ln(q_T^2/Q^2) + 3)$ is the well-known first-order contribution to the Sudakov form factor. The next two terms both contain the LO transversity splitting function δP_{qq}, convoluted with either the helicity parton distribution or the fragmentation function. A generic low-q_T structure with the Sudakov form factor and splitting functions is familiar from the spin-averaged case (see Ref. [71]). However, the appearance of the transversity splitting function in combination with Δf_q or D_q^h, and along with an overall factor C_A, is quite remarkable. This feature must be related to the fact that in the TMD framework the leading part of $A_{\rm UL}^{\sin\phi_h}$ receives contributions from the T-even function h_L, which is twist three and describes the distribution of transversely polarized quarks in a longitudinally polarized hadron, convoluted with the Collins function probing the fragmentation of transversely polarized quarks [38]. The last term in (25) and the results in Eqs. (27) and (29) do not appear to have a straightforward structure. Another striking feature is the appearance of a logarithm of q_T/Q in the result for the $g \to q$ channel in Eq. (29): Such logarithms do not usually appear in off-diagonal contributions at lowest order.

Similarly, we can consider the low-q_T/Q limit for the $\sin(2\phi_h)$ terms. Here, we find for the $q \to q$ channel:

$$\begin{aligned}(\Delta f_q \otimes C_{\rm UL}^{\sin 2\phi_h, q\to q} \otimes D_q^h)(x,z) &= -e_q^2 \frac{3}{4} C_A \left\{ -C_F\left(2\ln\left(\frac{q_T^2}{Q^2}\right) + 3\right)\Delta f_q(x) D_q^h(z) \ln\left(\frac{q_T^2}{Q^2}\right)\right. \\ &\quad \left. + D_q^h(z)\int_x^1 d\hat{x}\, \delta P_{qq}(\hat{x}) \Delta f_q\left(\frac{x}{\hat{x}}\right) + \Delta f_q(x)\int_z^1 d\hat{z}\, \delta P_{qq}(\hat{z}) D_q^h\left(\frac{z}{\hat{z}}\right)\right\} \\ &\quad + \frac{C_F}{2C_A}\Delta f_q(x)\int_z^1 d\hat{z}\frac{\hat{z}}{(1-\hat{z})^2}\left(1 - 3\hat{z} - 2(2\hat{z}-1)\frac{\ln\hat{z}}{1-\hat{z}}\right) D_q^h\left(\frac{z}{\hat{z}}\right).\end{aligned} \tag{31}$$

Apart from normalization, the first three terms are identical to the corresponding ones in Eq. (25). We note that, despite first appearances, the integrand of the last term is regular as $\hat{z} \to 1$.

In the $q \to g$ channel, we have

$$(\Delta f_q \otimes C_{\rm UL}^{\sin 2\phi_h, q\to g} \otimes D_g^h)(x,z) = -e_q^2 C_F \Delta f_q(x) \int_z^1 \frac{d\hat{z}}{\hat{z}} \left((C_A - 2C_F) \frac{(1-2\hat{z})\ln(1-\hat{z})}{\hat{z}} + (C_A - (2-3\hat{z})C_F) \right) D_g^h\left(\frac{z}{\hat{z}}\right). \tag{32}$$

For the channel $\gamma^* g \to q\bar{q}$, we again need the expansion (28) and obtain

$$(\Delta f_g \otimes C_{\rm UL}^{\sin 2\phi_h, g\to q} \otimes D_q^h)(x,z) = \frac{e_q^2}{2}(C_A - 2C_F) D_q^h(z) \int_x^1 d\hat{x}\, \Delta f_g\left(\frac{x}{\hat{x}}\right)\hat{x}\left[\ln\left(\frac{Q^2}{q_T^2}\right) + \ln\left(\frac{1-\hat{x}}{\hat{x}}\right) + \frac{3}{2}\right]. \tag{33}$$

The results in Eqs. (32) and (33) receive corrections of order q_T^2/Q^2 so that

$$F_{\rm UL}^{\sin 2\phi_h} \propto \frac{1}{Q^2} + \mathcal{O}\left(\frac{q_T^2}{Q^4}\right), \tag{34}$$

again up to logarithms.

Our low-q_T expansions fill two of the gaps reported in Table 2 of Ref. [47], providing the missing perturbative expressions for the ϕ_h-dependent T-odd cross sections. From the point of view of TMD factorization, they correspond to the leading part of the "high-q_T calculation." As discussed in [47], the TMD framework predicts the same behavior $\propto 1/(Qq_T)$ of the $\sin(\phi_h)$ terms as we find in Eq. (30). In this sense, the TMD calculation matches the collinear one. At this point, however, one cannot decide whether this matching is really quantitative in the sense that not just the overall power counting matches, but also the full combination of hard-scattering coefficients, parton distributions, and fragmentation functions. Currently, despite enormous progress in recent years [50–59], the high-transverse-momentum tails of TMDs are not understood at a sufficient level to obtain definitive results for $A_{\rm UL}$, especially in the case of the fragmentation correlators. Clearly, it will be very interesting to explore this issue more deeply in the future, also in the light of TMD factorization theorems extending beyond leading twist proposed recently [56,58].

For the $\sin(2\phi_h)$ terms, we find in Eq. (34) that the perturbative structure function becomes constant at low q_T. Including the factors of the strong coupling, $F_{\rm UL}^{\sin 2\phi_h}$ behaves in total as α_s^2/Q^2. This result is not in accordance with the TMD prediction [47] that the high-q_T tail of this structure function should behave as α_s/q_T^4. In the TMD framework, $F_{\rm UL}^{\sin 2\phi_h}$ is leading twist, being a convolution of the longitudinal worm-gear functions with Collins functions [38]. As one can see, even the powers of the strong coupling differ between the TMD prediction and our perturbative result.

In the context of this discussion, it is also interesting to recall the corresponding results for the T-odd beam spin asymmetry $A_{\rm LU}$ [16,17], for which the initial lepton is polarized. The relevant results are given in Appendix B. Interestingly, at low q_T, the same features as described above for $A_{\rm UL}$ are encountered.

VI. PHENOMENOLOGICAL RESULTS

We now present some simple phenomenology of the T-odd effects in SIDIS with longitudinally polarized protons. We will not carry out any full-fledged study; rather, we wish to explore the overall size of the $\sin\phi_h$ and $\sin(2\phi_h)$ modulations.

The quantities of interest in polarization experiments are typically spin asymmetries. In the present case, the longitudinal proton helicity single spin asymmetry in SIDIS is defined as

$$A_{\rm UL}(\phi_h) \equiv \frac{d\sigma_+^h(\phi_h) - d\sigma_-^h(\phi_h)}{d\sigma_+^h(\phi_h) + d\sigma_-^h(\phi_h)}, \tag{35}$$

where, as in Sec. II, $d\sigma_\pm^h$ represents the (differential) cross section for positive (negative) proton helicity. The denominator of the asymmetry is just twice the spin-averaged cross section as a function of the azimuthal angle ϕ_h. As is well known [38,69], this cross section has a ϕ_h independent piece as well as terms proportional to $\cos(\phi_h)$ and $\cos(2\phi_h)$. Dividing numerator and denominator by the ϕ_h independent term, we may write

$$A_{\rm UL}(\phi_h) = \frac{A_{\rm UL}^{\sin\phi_h}\sin\phi_h + A_{\rm UL}^{\sin 2\phi_h}\sin 2\phi_h}{1 + A_{UU}^{\cos\phi_h}\cos\phi_h + A_{UU}^{\cos 2\phi_h}\cos 2\phi_h}. \tag{36}$$

The various angular modulations $A_{\rm UL}^{\sin\phi_h}$ etc. are also known as analyzing powers. The ones of interest to us here, $A_{\rm UL}^{\sin\phi_h}$ and $A_{\rm UL}^{\sin 2\phi_h}$, may be extracted from the full cross section as follows:

$$A_{\rm UL}^{\sin n\phi_h} = \frac{\int_0^{2\pi} d\phi_h \sin(n\phi_h)[d\sigma_+^h(\phi_h) - d\sigma_-^h(\phi_h)]}{\frac{1}{2}\int_0^{2\pi} d\phi_h [d\sigma_+^h(\phi_h) + d\sigma_-^h(\phi_h)]} \quad (n = 1,2). \tag{37}$$

In this way, the terms with $\cos(\phi_h)$ and $\cos(2\phi_h)$ in the spin-averaged cross section do not contribute. Experimental data are commonly reported in terms of the $A_{\rm UL}^{\sin n\phi_h}$, and accordingly, these are the quantities that we will consider for our numerical predictions.

As stated earlier, in the present paper, we restrict ourselves to LO predictions for the T-odd terms, keeping the leading contribution $\propto \alpha_s^2$ in the numerator. For consistency, we therefore also need to use only the LO term in the denominator, which is only of order α_s and is easily computed [61]. (We note that the NLO corrections for the spin-averaged cross section in the denominator are available [72–74].) Because of this mismatch of perturbative orders in the numerator and denominator, the analyzing powers $A_{\rm UL}^{\sin\phi_h}, A_{\rm UL}^{\sin 2\phi_h}$ are themselves of order α_s, which is in contrast to most other spin asymmetries for which the leading power of α_s cancels. We therefore expect $A_{\rm UL}^{\sin\phi_h}, A_{\rm UL}^{\sin 2\phi_h}$ to be quite sensitive to the choice of scale and to higher-order corrections.

For our numerical studies, we use the DSSV [75,76] set for the helicity parton distributions and the DSS14 [77] set of fragmentation functions. We note that only pion fragmentation is considered in this set. We set the renormalization and factorization scales equal to Q. For the denominator of the asymmetries, we use the NNPDF31 [78] set of unpolarized parton distributions. We call this set from the LHAPDF library [79].

We start by presenting estimates for the future EIC with a center-of-mass energy of 140 GeV. At this fairly high energy, the $\sin\phi_h$ and $\sin(2\phi_h)$ modulations are overall quite strongly suppressed. The reason is that at high energies rather low, momentum fractions in the parton distribution functions are probed, where the polarized distributions are much smaller than the unpolarized ones. The left part of Fig. 5 shows x dependence of the analyzing powers $A_{\rm UL}^{\sin\phi_h}$ (blue solid line) and $-A_{\rm UL}^{\sin 2\phi_h}$ (red dashed line) for π^+ production, at a set of fixed values of z, Q^2, and $P_{h\perp}$. These values have been chosen by considering the "projected EIC data" shown in Ref. [34]. We observe that the asymmetries indeed rapidly decrease toward low values of x. The right part of the figure shows the z dependence of the asymmetries, which is much more moderate through most of the range considered.

In the following, we show results integrated over large bins in z and Q^2, but differential in $P_{h\perp}$ and x. To this end, we define

$$A_{UL,\rm int}^{\sin n\phi_h} \equiv \frac{\int_{z_{\rm min}}^{z_{\rm max}} dz \int_{Q^2_{\rm min}}^{Q^2_{\rm max}} dQ^2 \int_0^{2\pi} d\phi_h \sin(n\phi_h)[d\sigma^+(\phi_h) - d\sigma^-(\phi_h)]}{\frac{1}{2}\int_{z_{\rm min}}^{z_{\rm max}} dz \int_{Q^2_{\rm min}}^{Q^2_{\rm max}} dQ^2 \int_0^{2\pi} d\phi_h [d\sigma^+(\phi_h) + d\sigma^-(\phi_h)]} \quad (n = 1, 2). \tag{38}$$

Figure 6 shows $A_{UL,\rm int}^{\sin\phi_h}$ and $A_{UL,\rm int}^{\sin 2\phi_h}$ as functions of $P_{h\perp}$ at the EIC, for fixed values $x = 0.1$ (blue solid) and $x = 0.01$ (red dashed), for production of positive and negative pions. As expected for an $\mathcal{O}(\alpha_s)$ effect, and because of the suppression of the polarized parton distributions already mentioned, the asymmetries are quite small, especially for $x = 0.01$. Also, $A_{UL,\rm int}^{\sin 2\phi_h}$ is generally smaller than $A_{UL,\rm int}^{\sin\phi_h}$ because of its stronger suppression at low q_T/Q discussed in the previous section. We also observe that the asymmetries for positively and negatively charged pions tend to have opposite signs, which is due to the dominance of the (positive) up-quark helicity parton distribution for π^+ production and of the (negative) down-quark helicity distribution in case of π^-. We note that detailed studies

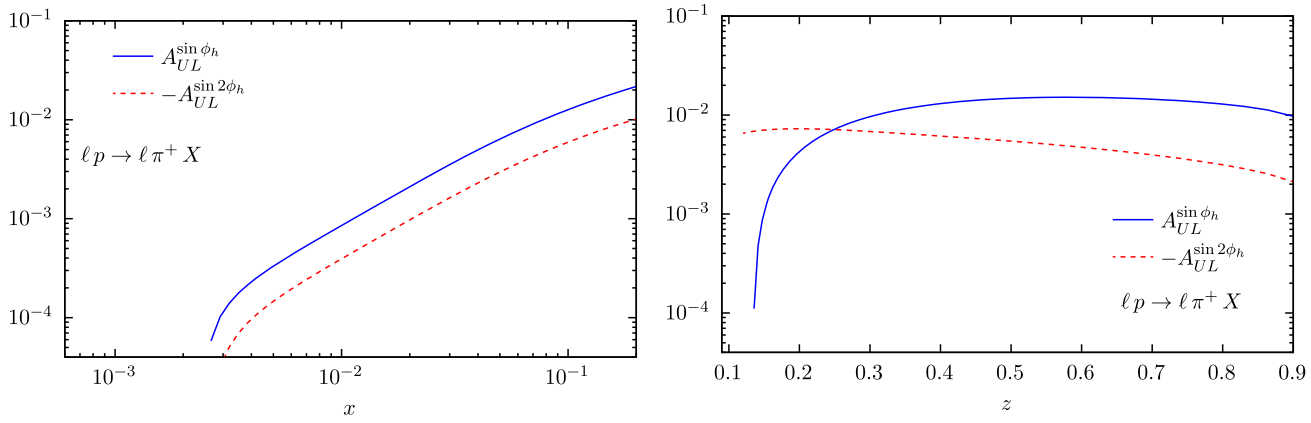

FIG. 5. Left: x dependence and Right: z dependence of the analyzing powers for $\ell p \to \ell \pi^+ X$ at the future EIC. The $\sin(2\phi_h)$ analyzing power has been multiplied by (-1). For the left graph, $z = 0.4$, while for the right graph, $x = 0.1$. In both cases, we use $\sqrt{s} = 140$ GeV, $Q^2 = 50$ GeV^2, and $P_{h\perp} = 2$ GeV.

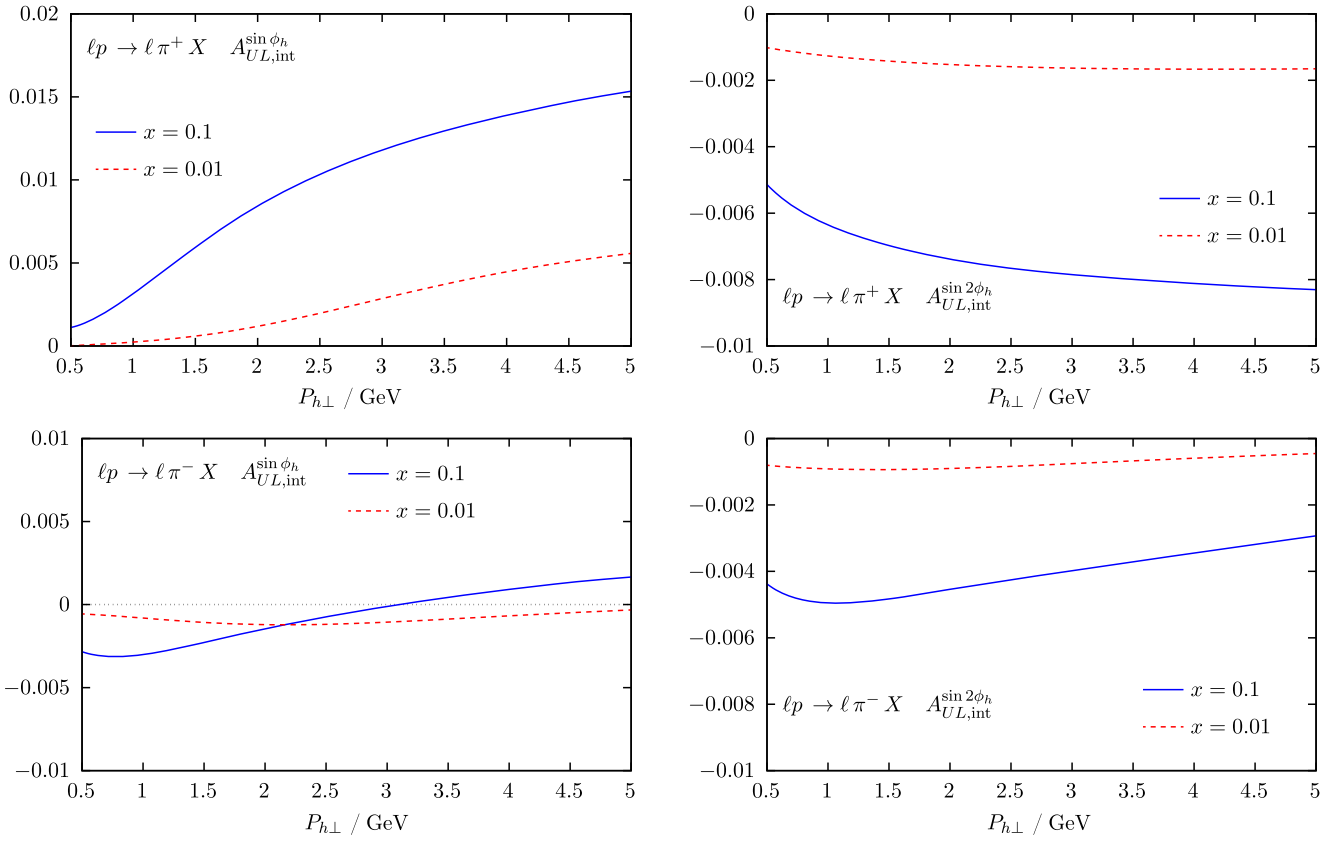

FIG. 6. T-odd asymmetries as functions of $P_{h\perp}$ for $x = 0.1$ and $x = 0.01$ for $\ell p \to \ell \pi^+ X$ and $\ell p \to \ell \pi^- X$ at the EIC. We have integrated the cross sections over $Q^2/(\mathrm{GeV})^2 \in [10, 100]$ for $x = 0.1$ (blue solid) and $Q^2/(\mathrm{GeV})^2 \in [2, 10]$ for $x = 0.01$ (red dashed), and in both cases over $z \in [0.05, 0.8]$.

of the uncertainties to be expected for such measurements at the EIC will evidently require a full analysis that also incorporates efficiencies and detector effects, which is beyond the scope of our paper. A ballpark estimate based on the spin-averaged SIDIS rates expected at the EIC (as reported in [34]) provides confidence that even asymmetries of the small size as in Fig. 6 should be resolvable at the EIC.

We proceed by presenting a comparison to data from COMPASS [31] where the asymmetry A_{UL} has been measured in muon scattering off longitudinally polarized deuterons at $\sqrt{s} = 17.4$ GeV. Such a comparison is of course somewhat precarious as the hadron transverse momenta accessed in the COMPASS SIDIS data are typically below 1 GeV. Even though Q^2 extends to values well in the perturbative regime and $q_T = P_{h\perp}/z$ is typically significantly larger than 1 GeV, it is clear that the use of perturbation theory is questionable. Arguably a TMD description would appear to be more appropriate here. Related to this, for a valid perturbative description, one should address the Sudakov logarithms we have found at low q_T (see Sec. V) and resum them to all orders of perturbation theory. Such an analysis is presently not possible since the evolution of all TMD functions contributing to A_{UL} is not yet available. In any case, our main interest here is to explore the rough size of the perturbative predictions for A_{UL} and to see whether there is broad consistency with the experimental data.

We note that COMPASS has considered the production of arbitrary charged hadrons. Sets of fragmentation functions for $h^{\pm}$ are not available in DSS14, so we continue to use the pion fragmentation functions. Given that pions dominate the spectrum of produced hadrons and that fragmentation effects cancel to some extent in the spin asymmetry, this should be more than sufficient for a first comparison. We consider the π^+-channel: $\mu d \to \mu \pi^+ X$. As in [31], we integrate over $x \in [0.004, 0.7]$, $z \in [0.01, 1]$, and $Q^2/(\mathrm{GeV})^2 \in [1, 100]$ and divide by the value $|P_L| = 0.8$ of the muon beam polarization. Figure 7 shows the comparisons both for $A_{\mathrm{UL}}^{\sin\phi_h}$ and for $A_{\mathrm{UL}}^{\sin 2\phi_h}$. We observe reasonable agreement, given the rather large uncertainties of the data and keeping in mind that the $P_{h\perp}$ values are such that a TMD description would appear to be more appropriate as discussed above.

We finally also show a comparison to data from the HERMES experiment [26,29] taken for $\pi^{\pm}$ production at $\sqrt{s} = 7.25$ GeV. As we discussed in Sec. II, in an actual

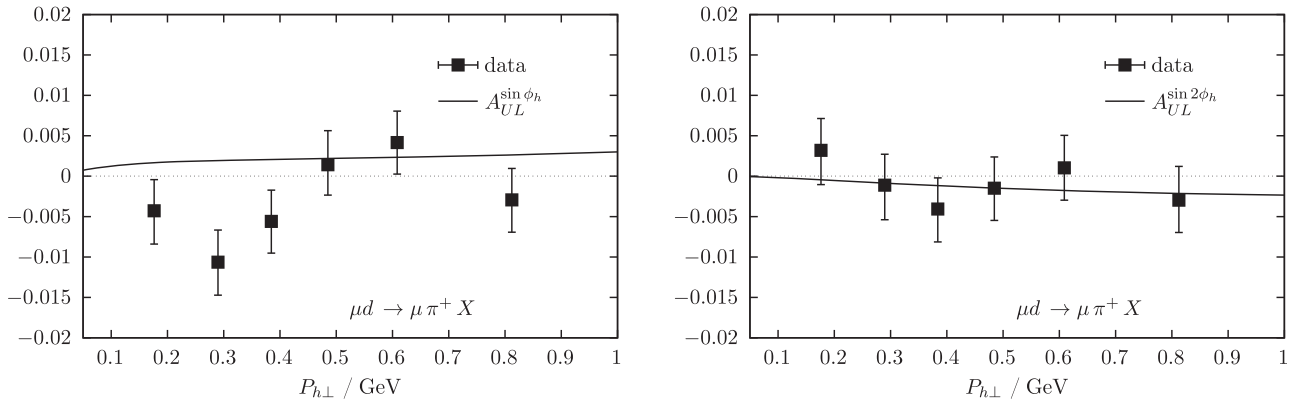

FIG. 7. Comparison of our numerical estimates for $A_{\mathrm{UL}}^{\sin\phi_h}$ and $A_{\mathrm{UL}}^{\sin 2\phi_h}$ with data from the COMPASS collaboration [31] in hadron production off longitudinally polarized deuterons at $\sqrt{s} = 17.4$ GeV. We show the $P_{h\perp}$ distribution of the asymmetry integrated over $x \in [0.004, 0.7]$, $z \in [0.01, 1]$, and $Q^2/(\mathrm{GeV})^2 \in [1, 100]$.

experiment, the target is polarized along (or opposite to) the lepton beam direction. This means that the measured asymmetry A_{UL} receives contributions from both the longitudinal and transverse spin asymmetries with respect to the direction of the virtual photon [29,60] so that $A_{\mathrm{UL}}(l) \neq A_{\mathrm{UL}}(q)$ (where the arguments l and q denote target polarization defined relative to the lepton or photon direction, respectively). For HERMES with its relatively modest Q^2 values, the difference between $A_{\mathrm{UL}}(l)$ and $A_{\mathrm{UL}}(q)$—which is of subleading twist—is expected to be potentially more pronounced. Combining with data taken with a transversely polarized target, HERMES has in fact been able to provide an extraction of $A_{\mathrm{UL}}(q)$ [29]. Figure 8 shows both sets of HERMES data, $A_{\mathrm{UL}}^{\sin\phi_h}(l)$ and $A_{\mathrm{UL}}^{\sin\phi_h}(q)$, compared to our calculations of $A_{\mathrm{UL}}^{\sin\phi_h}(q)$. We show the comparisons as functions of x and z, using the mean values of x, z, Q^2, and $P_{h\perp}$ for each point reported in Table 1 of [29]. One can see that for positively charged pions, the differences between $A_{\mathrm{UL}}^{\sin\phi_h}(l)$ and $A_{\mathrm{UL}}^{\sin\phi_h}(q)$ are quite large,

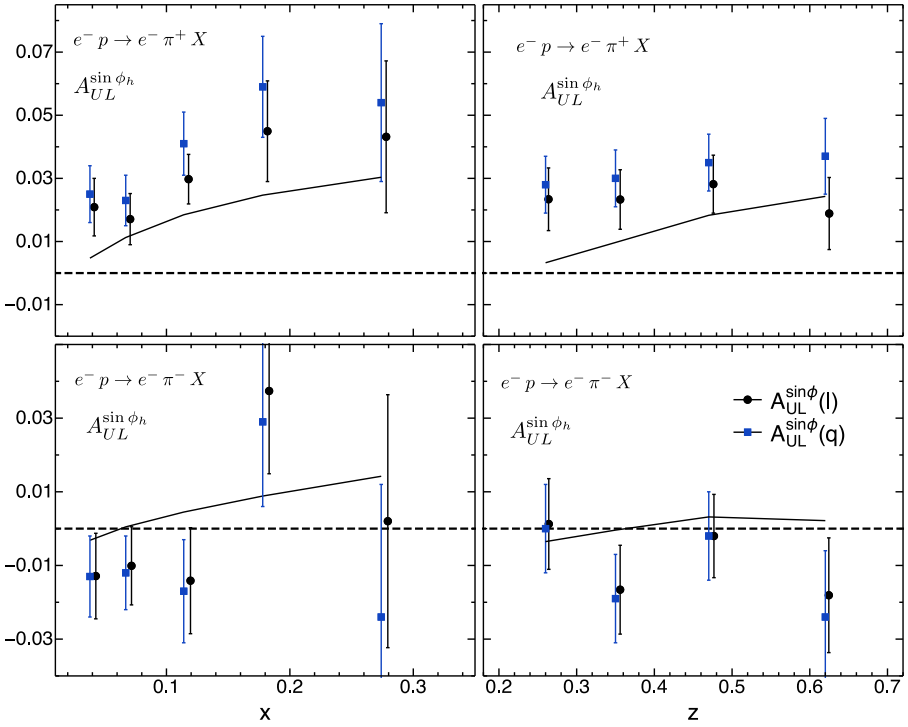

FIG. 8. Comparison of our calculations of $A_{\mathrm{UL}}^{\sin\phi_h}$ with data from the HERMES collaboration [29] in $\pi^{\pm}$ production off longitudinally polarized protons, as functions of x (left) and z (right). $A_{\mathrm{UL}}^{\sin\phi_h}(l)$ and $A_{\mathrm{UL}}^{\sin\phi_h}(q)$ represent the asymmetries for target polarization defined relative to the lepton or photon direction, respectively.

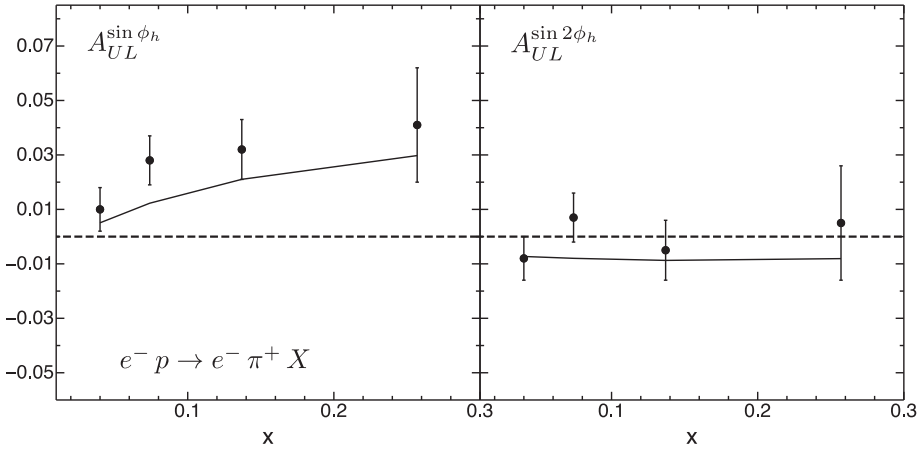

FIG. 9. Numerical results for $A_{\mathrm{UL}}^{\sin\phi_h}$ and $A_{\mathrm{UL}}^{\sin 2\phi_h}$ compared to HERMES data [26] for π^+ production off longitudinally polarized protons. The data have not been corrected for the polarization direction.

while they are small for π^- production. We also notice that our calculations reproduce the trend of the data rather well overall, despite the fact that HERMES accessed only rather small transverse momenta.

HERMES data for the $\sin 2\phi_h$ asymmetry are available only without correction for the polarization direction [26]. The right part of Fig. 9 shows the data for $A_{\mathrm{UL}}^{\sin 2\phi_h}(l)$ for π^+ production, compared to our calculations. Here, we have used the mean values of x and Q^2 for each point as given in [26], while adopting $\langle z\rangle$ and $\langle P_{h\perp}\rangle$ from [29]. To facilitate comparison with the $\sin\phi_h$ asymmetry, we show the corresponding results for $A_{\mathrm{UL}}^{\sin\phi_h}$ on the left side of Fig. 9. As before, the $\sin 2\phi_h$ asymmetry is smaller. Our calculations are overall in fair agreement with the data for both asymmetries; in particular, they nicely capture the difference in magnitude between the $\sin\phi_h$ and $\sin 2\phi_h$ components. The situation thus appears to be different from that for the $\cos 2\phi_h$ unpolarized structure function $F_{UU}^{\cos 2\phi_h}$ analyzed in [80], for which the perturbative $\mathcal{O}(\alpha_s)$ prediction for HERMES kinematics was shown to be negligible compared to higher-twist effects. It should be stressed again, however, that the data shown in Fig. 9 have not been corrected for the polarization direction, and according to Fig. 8, such correction effects are expected to be particularly important in the case of π^+ production.

VII. CONCLUSIONS

We have presented a perturbative calculation for the single-spin asymmetry A_{UL} in semi-inclusive deep-inelastic scattering, which may be measured by scattering unpolarized leptons off longitudinally polarized nucleons. This asymmetry is interesting because, in the absence of parity violation, it is T-odd and receives perturbative contributions only via QCD loop effects. Also, it is sensitive to the proton's helicity parton distributions, despite the fact that it is measured with an unpolarized lepton beam. Our calculation builds on the large body of previous work on T-odd effects in hard scattering, opening a new avenue for future measurements at the EIC.

We have provided compact expressions for the T-odd contributions in the various partonic channels. We have used these to derive the low-transverse-momentum behavior of the T-odd terms, which shows striking features. Our results add new information on the relations between TMDs and perturbative hard scattering, which had been missing so far. They may be used for comparisons to detailed quantitative predictions to be obtained in the future within the TMD formalism.

Our phenomenological calculations reveal the expected relatively small size of the T-odd asymmetries. We have made predictions for the asymmetries at the future EIC, where it should be possible to explore them. Our results are also broadly consistent with available COMPASS and HERMES data, although the applicability of a purely hard-scattering picture is questionable here. All in all, we hope that our paper will contribute to the long-standing quest to establish and understand T-odd effects in QCD.

ACKNOWLEDGMENTS

We thank A. Bacchetta, M. Diehl, Y. Hatta, M. Schlegel, and A. Vladimirov for useful discussions. A. S. is grateful to the University of the Basque Country, Bilbao, for hospitality. This study was supported in part by Deutsche Forschungsgemeinschaft (DFG) through the Research Unit FOR 2926.

APPENDIX A: DERIVATION OF EQ. (28)

Setting $\rho \equiv q_T^2/Q^2$, we consider the expression,

$$\begin{aligned}
&\int_x^1 \frac{d\hat{x}}{\hat{x}} \int_z^1 \frac{d\hat{z}}{\hat{z}} \ln(1-\hat{z}) \delta\left(\rho - \frac{(1-\hat{x})(1-\hat{z})}{\hat{x}\,\hat{z}}\right) \Delta f\left(\frac{x}{\hat{x}}\right) D\left(\frac{z}{\hat{z}}\right) \\
&= \int_x^{\frac{1-z}{1-z(1-\rho)}} d\hat{x} \left\{ \frac{\ln(1-\hat{z})}{1-\hat{x}(1-\rho)} \Delta f\left(\frac{x}{\hat{x}}\right) D\left(\frac{z}{\hat{z}}\right) \right\}_{\hat{z}=\frac{1-\hat{x}}{1-\hat{x}(1-\rho)}} \\
&= \int_x^{\frac{1-z}{1-z(1-\rho)}} d\hat{x} \frac{\ln\left(\frac{\rho\hat{x}}{1-\hat{x}(1-\rho)}\right)}{1-\hat{x}(1-\rho)} \left[\left(\Delta f\left(\frac{x}{\hat{x}}\right) - \Delta f(x) \right) \left(D\left(\frac{z}{\hat{z}}\right) - D(z) \right) \right. \\
&\quad \left. + D(z) \left(\Delta f\left(\frac{x}{\hat{x}}\right) - \Delta f(x) \right) + \Delta f(x) \left(D\left(\frac{z}{\hat{z}}\right) - D(z) \right) + \Delta f(x) D(z) \right]_{\hat{z}=\frac{1-\hat{x}}{1-\hat{x}(1-\rho)}}.
\end{aligned} \tag{A1}$$

In the second equality, we have added and subtracted terms in such a way that four types of contributions arise. The first one with $(\Delta f(x/\hat{x}) - \Delta f(x))(D(z/\hat{z}) - D(z))$ is easily seen to vanish for $q_T/Q \to 0$ since $\hat{z} \to 1$ in that limit. The second term becomes, at small ρ,

$$\begin{aligned}
D(z) \int_x^{\frac{1-z}{1-z(1-\rho)}} d\hat{x} \frac{\ln\left(\frac{\rho\hat{x}}{1-\hat{x}(1-\rho)}\right)}{1-\hat{x}(1-\rho)} \left(\Delta f\left(\frac{x}{\hat{x}}\right) - \Delta f(x) \right) &= D(z) \int_x^1 d\hat{x} \left[\left(\frac{\ln\rho - \ln(1-\hat{x})}{1-\hat{x}} \right)_+ + \frac{\ln\hat{x}}{1-\hat{x}} \right] \Delta f\left(\frac{x}{\hat{x}}\right) \\
&\quad + D(z) \Delta f(x) \left(\frac{1}{2}\ln^2(1-x) - \ln\rho \ln(1-x) + \mathrm{Li}_2(1-x) \right) + \mathcal{O}(\rho),
\end{aligned} \tag{A2}$$

where the plus distribution is defined as in Eq. (23) and where Li_2 denotes the dilogarithm function. For the third term, we go back to $\hat{z}$ as integration variable. We then find

$$\Delta f(x) \int_z^{\frac{1-x}{1-x(1-\rho)}} d\hat{z} \frac{\ln(1-\hat{z})}{1-\hat{z}(1-\rho)} \left(D\left(\frac{z}{\hat{z}}\right) - D(z) \right) = \Delta f(x) \int_z^1 d\hat{z} \left(\frac{\ln(1-\hat{z})}{1-\hat{z}} \right)_+ D\left(\frac{z}{\hat{z}}\right) - \frac{1}{2}\ln^2(1-z) \Delta f(x) D(z) + \mathcal{O}(\rho). \tag{A3}$$

Finally, for the last term in (A1), we obtain

$$\begin{aligned}
\Delta f(x) D(z) \int_x^{\frac{1-z}{1-z(1-\rho)}} d\hat{x} \frac{\ln\left(\frac{\rho\hat{x}}{1-\hat{x}(1-\rho)}\right)}{1-\hat{x}(1-\rho)} &= \Delta f(x) D(z) \left\{ -\frac{1}{2}\ln^2(\rho) + \ln\rho \ln(1-x) \right. \\
&\quad \left. - \frac{1}{2}\ln^2(1-x) + \frac{1}{2}\ln^2(1-z) - \mathrm{Li}_2(1-x) \right\} + \mathcal{O}(\rho).
\end{aligned} \tag{A4}$$

Combining all terms in (A2)–(A4) and expressing them in terms of distributions, we directly recover Eq. (28). Note that all terms involving logarithms or dilogarithms of the lower integration limits x, z cancel in the final answer, as they should, since we have defined our plus distributions by integrations from 0 to 1 [see Eq. (23)].

APPENDIX B: PERTURBATIVE RESULTS FOR THE BEAM-SPIN ASYMMETRY A_{LU}

The cross section for the beam-spin asymmetry A_{LU} may be written as [38]

$$\frac{d^5\Delta\sigma^h}{dxdydzdP_{h\perp}^2 d\phi_h} = \frac{1}{2}\left(\frac{d^5\sigma_+^h}{dxdydzdP_{h\perp}^2 d\phi_h} - \frac{d^5\sigma_-^h}{dxdydzdP_{h\perp}^2 d\phi_h}\right) = \frac{\pi\alpha^2 y}{xQ^2}\sqrt{\frac{2\varepsilon}{1-\varepsilon}}F_{\mathrm{LU}}^{\sin\phi_h}\sin(\phi_h). \tag{B1}$$

As is well-known, there is no term with $\sin(2\phi_h)$ for single-photon exchange. Writing the structure function $F_{\mathrm{LU}}^{\sin\phi_h}$ as

$$F_{\mathrm{LU}}^{\sin\phi_h} = \left(\frac{\alpha_s(\mu^2)}{2\pi}\right)^2 \frac{x}{Q^2 z^2}\sum_{\substack{a,b\\=q,\bar{q},g}}\int_x^1\frac{d\hat{x}}{\hat{x}}\int_z^1\frac{d\hat{z}}{\hat{z}}\Delta f_a\left(\frac{x}{\hat{x}},\mu^2\right)C_{\mathrm{LU}}^{\sin\phi_h,a\to b}(\hat{x},\hat{z})D_b^h\left(\frac{z}{\hat{z}},\mu^2\right)\delta\left(\frac{q_T^2}{Q^2}-\frac{(1-\hat{x})(1-\hat{z})}{\hat{x}\,\hat{z}}\right), \tag{B2}$$

we have from Refs. [10,17]:

$$\begin{aligned}
C_{\mathrm{LU}}^{\sin\phi_h,q\to q}(\hat{x},\hat{z}) &= -e_q^2 C_F\left(C_A(1-\hat{x}) - C_F(1-\hat{x}+\hat{z}+\hat{x}\,\hat{z}) + (C_A-2C_F)\frac{\hat{z}\ln\hat{z}}{1-\hat{z}}\right)\frac{Q}{q_T},\\
C_{\mathrm{LU}}^{\sin\phi_h,q\to g}(\hat{x},\hat{z}) &= e_q^2 C_F\frac{(1-\hat{z})}{\hat{z}}\left(C_A(1-\hat{x}) + C_F(\hat{x}\,\hat{z}+\hat{z}-2) + (C_A-2C_F)\frac{(1-\hat{z})\ln(1-\hat{z})}{\hat{z}}\right)\frac{Q}{q_T},\\
C_{\mathrm{LU}}^{\sin\phi_h,g\to q}(\hat{x},\hat{z}) &= -e_q^2(C_A-2C_F)\frac{1-\hat{x}}{2\hat{z}^2}\left(-\hat{x}\,\hat{z}(1-2\hat{z}) - (1-\hat{x})\ln(1-\hat{z}) + (1-\hat{x})\frac{\hat{z}\ln(\hat{z})}{1-\hat{z}}\right)\frac{Q}{q_T}.
\end{aligned} \tag{B3}$$

Carrying out the expansions for low q_T/Q we find, up to corrections of order q_T/Q,

$$\begin{aligned}
(f_q\otimes C_{\mathrm{LU}}^{\sin\phi_h,q\to q}\otimes D_q^h)(x,z) &= e_q^2\frac{Q}{q_T}\frac{C_A}{2}\left\{-C_F\left(2\ln\left(\frac{q_T^2}{Q^2}\right)+3\right)f_q(x)D_q^h(z) + D_q^h(z)\int_x^1 d\hat{x}\,\delta P_{qq}(\hat{x})f_q\left(\frac{x}{\hat{x}}\right)\right.\\
&\left. + f_q(x)\int_z^1 d\hat{z}\,\delta P_{qq}(\hat{z})D_q^h\left(\frac{z}{\hat{z}}\right)\right\} - e_q^2\frac{Q}{q_T}\frac{C_F}{C_A}f_q(x)\int_z^1 d\hat{z}\frac{\hat{z}}{1-\hat{z}}\left(1+\frac{\ln\hat{z}}{1-\hat{z}}\right)D_q^h\left(\frac{z}{\hat{z}}\right),\\
(f_q\otimes C_{\mathrm{LU}}^{\sin\phi_h,q\to g}\otimes D_g^h)(x,z) &= e_q^2\frac{Q}{q_T}C_F f_q(x)\int_z^1 d\hat{z}\frac{1-\hat{z}}{\hat{z}^2}((C_A-2C_F)\ln(1-\hat{z}) - 2C_F\hat{z})D_g^h\left(\frac{z}{\hat{z}}\right),\\
(f_g\otimes C_{\mathrm{LU}}^{\sin\phi_h,g\to q}\otimes D_q^h)(x,z)] &= -\frac{e_q^2}{2}\frac{Q}{q_T}(C_A-2C_F)D_q^h(z)\int_x^1 d\hat{x}\,f_g\left(\frac{x}{\hat{x}}\right)\left[(1-\hat{x})\ln\left(\frac{Q^2}{q_T^2}\right) + (1-\hat{x})\ln\left(\frac{1-\hat{x}}{\hat{x}}\right) + 2x - 1\right],
\end{aligned} \tag{B4}$$

where the convolution has been defined in (24) and the transversity splitting function in (26).

[1] For review, see: M. Grosse Perdekamp and F. Yuan, Annu. Rev. Nucl. Part. Sci. **65**, 429 (2015).
[2] D. W. Sivers, Phys. Rev. D **41**, 83 (1990).
[3] S. J. Brodsky, D. S. Hwang, and I. Schmidt, Phys. Lett. B **530**, 99 (2002).
[4] J. C. Collins, Phys. Lett. B **536**, 43 (2002).
[5] A. De Rujula, J. M. Kaplan, and E. De Rafael, Nucl. Phys. **B35**, 365 (1971).
[6] A. De Rujula, R. Petronzio, and B. E. Lautrup, Nucl. Phys. **B146**, 50 (1978).
[7] K. Fabricius, I. Schmitt, G. Kramer, and G. Schierholz, Phys. Rev. Lett. **45**, 867 (1980).
[8] J. G. Körner, G. Kramer, G. Schierholz, K. Fabricius, and I. Schmitt, Phys. Lett. **94B**, 207 (1980).
[9] K. Hagiwara, K. i. Hikasa, and N. Kai, Phys. Rev. Lett. **47**, 983 (1981).

[10] K. Hagiwara, K. i. Hikasa, and N. Kai, Phys. Rev. D **27**, 84 (1983).
[11] B. Pire and J. P. Ralston, Phys. Rev. D **28**, 260 (1983).
[12] K. Hagiwara, K. i. Hikasa, and N. Kai, Phys. Rev. Lett. **52**, 1076 (1984).
[13] A. Bilal, E. Masso, and A. De Rujula, Nucl. Phys. **B355**, 549 (1991).
[14] R. D. Carlitz and R. S. Willey, Phys. Rev. D **45**, 2323 (1992).
[15] A. Brandenburg, L. J. Dixon, and Y. Shadmi, Phys. Rev. D **53**, 1264 (1996).
[16] M. Ahmed and T. Gehrmann, Phys. Lett. B **465**, 297 (1999).
[17] J. G. Körner, B. Melic, and Z. Merebashvili, Phys. Rev. D **62**, 096011 (2000).
[18] K. Hagiwara, K. Mawatari, and H. Yokoya, J. High Energy Phys. 12 (2007) 041.
[19] R. Frederix, K. Hagiwara, T. Yamada, and H. Yokoya, Phys. Rev. Lett. **113**, 152001 (2014).
[20] S. Benic, Y. Hatta, H. n. Li, and D. J. Yang, Phys. Rev. D **100**, 094027 (2019).
[21] S. Benić, Y. Hatta, A. Kaushik, and H. n. Li, Phys. Rev. D **104**, 094027 (2021).
[22] M. Aicher, Ph.D. thesis, Universität Regensburg, 2011.
[23] M. Abele, M.Sc. thesis, University of Tübingen, 2019.
[24] F. Piacenza, Ph.D. thesis, Università di Pavia, 2020.
[25] J. w. Qiu and G. F. Sterman, Phys. Rev. D **59**, 014004 (1998).
[26] A. Airapetian *et al.* (HERMES Collaboration), Phys. Rev. Lett. **84**, 4047 (2000).
[27] A. Airapetian *et al.* (HERMES Collaboration), Phys. Rev. D **64**, 097101 (2001).
[28] A. Airapetian *et al.* (HERMES Collaboration), Phys. Lett. B **562**, 182 (2003).
[29] A. Airapetian *et al.* (HERMES Collaboration), Phys. Lett. B **622**, 14 (2005).
[30] H. Avakian *et al.* (CLAS Collaboration), Phys. Rev. Lett. **105**, 262002 (2010).
[31] C. Adolph *et al.* (COMPASS Collaboration), Eur. Phys. J. C **78**, 952 (2018); **80**, 298(E) (2020).
[32] I. A. Savin (COMPASS Collaboration), J. Phys. Conf. Ser. **678**, 012063 (2016).
[33] M. G. Alekseev *et al.* (COMPASS Collaboration), Eur. Phys. J. C **70**, 39 (2010).
[34] E. C. Aschenauer, I. Borsa, R. Sassot, and C. Van Hulse, Phys. Rev. D **99**, 094004 (2019).
[35] T. C. Rogers, Eur. Phys. J. A **52**, 153 (2016).
[36] R. Angeles-Martinez, A. Bacchetta, I. I. Balitsky, D. Boer, M. Boglione, R. Boussarie, F. A. Ceccopieri, I. O. Cherednikov, P. Connor, M. G. Echevarria *et al.*, Acta Phys. Pol. B **46**, 2501 (2015).
[37] A. Bacchetta, P. J. Mulders, and F. Pijlman, Phys. Lett. B **595**, 309 (2004).
[38] A. Bacchetta, M. Diehl, K. Goeke, A. Metz, P. J. Mulders, and M. Schlegel, J. High Energy Phys. 02 (2007) 093.
[39] M. Boglione and P. J. Mulders, Phys. Lett. B **478**, 114 (2000).
[40] B. Q. Ma, I. Schmidt, and J. J. Yang, Phys. Rev. D **63**, 037501 (2001).
[41] B. Q. Ma, I. Schmidt, and J. J. Yang, Phys. Rev. D **65**, 034010 (2002).
[42] A. V. Efremov, K. Goeke, and P. Schweitzer, Phys. Lett. B **568**, 63 (2003).
[43] S. Boffi, A. V. Efremov, B. Pasquini, and P. Schweitzer, Phys. Rev. D **79**, 094012 (2009).
[44] J. Zhu and B. Q. Ma, Phys. Lett. B **696**, 246 (2011).
[45] Z. Lu, B. Q. Ma, and J. She, Phys. Rev. D **84**, 034010 (2011).
[46] H. Li and Z. Lu, arXiv:2111.03840.
[47] A. Bacchetta, D. Boer, M. Diehl, and P. J. Mulders, J. High Energy Phys. 08 (2008) 023.
[48] F. Yuan, Phys. Lett. B **589**, 28 (2004).
[49] A. V. Afanasev and C. E. Carlson, Phys. Rev. D **74**, 114027 (2006).
[50] X. Ji, J. W. Qiu, W. Vogelsang, and F. Yuan, Phys. Rev. Lett. **97**, 082002 (2006).
[51] X. Ji, J. W. Qiu, W. Vogelsang, and F. Yuan, Phys. Lett. B **638**, 178 (2006).
[52] F. Yuan and J. Zhou, Phys. Rev. Lett. **103**, 052001 (2009).
[53] K. Kanazawa, Y. Koike, A. Metz, D. Pitonyak, and M. Schlegel, Phys. Rev. D **93**, 054024 (2016).
[54] V. Moos and A. Vladimirov, J. High Energy Phys. 12 (2020) 145.
[55] I. Scimemi, A. Tarasov, and A. Vladimirov, J. High Energy Phys. 05 (2019) 125.
[56] A. Vladimirov, V. Moos, and I. Scimemi, J. High Energy Phys. 01 (2022) 110.
[57] I. Scimemi and A. Vladimirov, Eur. Phys. J. C **78**, 802 (2018).
[58] M. A. Ebert, A. Gao, and I. W. Stewart, J. High Energy Phys. 06 (2022) 007.
[59] S. Rodini and A. Vladimirov, arXiv:2204.03856.
[60] M. Diehl and S. Sapeta, Eur. Phys. J. C **41**, 515 (2005).
[61] A. Mendez, Nucl. Phys. **B145**, 199 (1978).
[62] G. Karpman, R. Leonardi, and F. Strocchi, Phys. Rev. **174**, 1957 (1968).
[63] F. Cannata, R. Leonardi, and F. Strocchi, Phys. Rev. D **1**, 191 (1970).
[64] G. 't Hooft and M. J. G. Veltman, Nucl. Phys. **B44**, 189 (1972).
[65] P. Breitenlohner and D. Maison, Commun. Math. Phys. **52**, 11 (1977).
[66] M. Jamin and M. E. Lautenbacher, Comput. Phys. Commun. **74**, 265 (1993).
[67] H. H. Patel, Comput. Phys. Commun. **218**, 66 (2017).
[68] S. Wandzura and F. Wilczek, Phys. Lett. B **72**, 195 (1977).
[69] R. b. Meng, F. I. Olness, and D. E. Soper, Nucl. Phys. **B371**, 79 (1992).
[70] R. Meng, F. I. Olness, and D. E. Soper, Phys. Rev. D **54**, 1919 (1996).
[71] D. Boer and W. Vogelsang, Phys. Rev. D **74**, 014004 (2006).
[72] A. Daleo, D. de Florian, and R. Sassot, Phys. Rev. D **71**, 034013 (2005).
[73] B. A. Kniehl, G. Kramer, and M. Maniatis, Nucl. Phys. **B711**, 345 (2005); **B720**, 231(E) (2005).
[74] B. Wang, J. O. Gonzalez-Hernandez, T. C. Rogers, and N. Sato, Phys. Rev. D **99**, 094029 (2019).
[75] D. de Florian, R. Sassot, M. Stratmann, and W. Vogelsang, Phys. Rev. Lett. **101**, 072001 (2008).

[76] D. de Florian, R. Sassot, M. Stratmann, and W. Vogelsang, Phys. Rev. D **80**, 034030 (2009).
[77] D. de Florian, R. Sassot, M. Epele, R. J. Hernández-Pinto, and M. Stratmann, Phys. Rev. D **91**, 014035 (2015).
[78] R. D. Ball *et al.* (NNPDF Collaboration), Eur. Phys. J. C **77**, 663 (2017).
[79] A. Buckley, J. Ferrando, S. Lloyd, K. Nordström, B. Page, M. Rüfenacht, M. Schönherr, and G. Watt, Eur. Phys. J. C **75**, 132 (2015).
[80] V. Barone, A. Prokudin, and B. Q. Ma, Phys. Rev. D **78**, 045022 (2008).